- Technical Paper -

SHEAR FAILURE MECHANISM OF SEGMENTAL CONCRETE BEAMS PRESTRESSED WITH EXTERNAL TENDONS

Chunyakom SIVALEEPUNTH[*1], Junichiro NIWA[*2], Dinh Hung NGUYEN[*3] and Yuzuru HAMADA[*4]

ABSTRACT

This paper describes the results of an experimental study and nonlinear FEM in order to examine the shear failure mechanism of segmental beams by varying the segmental length. The parametric study on the influence of loading position on the shear transfer is performed. It is found that the segmental length and loading position have less effect in shear carrying capacity of segmental beams. The experimental results are also compared with the simplified truss model and M_{cr} method for shear carrying capacity. The results from the simplified truss model agree well with the experiment.

Keywords: shear carrying capacity, simplified truss model, precast, prestressed concrete, external tendon

1. INTRODUCTION

Prefabricated segmental concrete bridges with external prestressing have been firstly developed with a span-by-span construction technique that is thought to be the simplest and fastest among this type of construction technique. For the construction of each of the spans, the segments are placed one next to the other with epoxy joint, suspended from an erection girder, and are post-tensioned with external tendons. Due to the popularity of segmental concrete structures, an examination of the design and analysis for shear carrying capacity of such structures is required.

The prediction of shear carrying capacity of externally prestressed monolithic concrete beams by the simplified truss model has already been presented in Sivaleepunth, C. et al. [1]. For evaluating the shear carrying capacity of slender prestressed concrete beams (shear span to effective depth ratio, a/d, is greater than or equal to 2.5.), predicted to fail in the shear compressive mode of failure, Sivaleepunth, C. et al. [1] conducted the parametric study by using the nonlinear finite element method (FEM). The influential parameters, such as lower fiber stress, upper fiber stress, compressive strength of concrete, shear span to effective depth ratio were found to have a significant effect on the change of the inclination of concentrated stress flow in a web, which is a key to solve the problem of shear compression failure mode. The simplified truss model was found to be able to predict the experimental results of several externally prestressed concrete monolithic beams very well. However, due to the discontinuity of segmental concrete beams, the simplified truss model may not be able to predict the shear carrying capacity, especially in the cases when the segmental joints opened. The shear transfer across opened joints is more complex.

The objectives of this study were (a) to investigate the shear failure mechanism of segmental concrete beams prestressed with external tendons by varying the segmental length, (b) to examine the influence of loading position, in order to simulate the practical loading condition, on the shear transfer in segmental concrete beams, (c) to check the accuracy of the simplified truss model [1] and M_{cr} Method [2] for evaluating the shear carrying capacity and (d) to investigate the accuracy in the prediction of critical crack from the simplified truss model.

2. LITERATURE REVIEWS

Due to the comprehensive explanation for the failure mechanism of prestressed concrete beams, the simplified truss model [1] is adopted in this study. The schematic diagram of the simplified truss model for analyzing the shear carrying capacity of externally prestressed concrete beams is illustrated in Fig. 1. The parameter m is used in the model to represent the inverse of slope of concentrated stress flow, where $m = \cot\theta$ and θ is the angle of the concentrated stress flow. The distance md is adopted as the horizontal distance from the loading point to the ended node of the diagonal compression member {3}, because most of the prestressed concrete beams have the concentrated stress flow along the diagonal compression member {3}. For the distance in horizontal direction from the loading point to the ended node of diagonal compression member {4} is set to be $0.5md$ due to the substress flow that occurs between the loading point to the ended node of diagonal compression member {3}; therefore, a half

*1 PhD. Candidate, Graduate School of Civil Engineering, Tokyo Institute of Technology, JCI Member
*2 Prof., Dept. of Civil Engineering, Tokyo Institute of Technology, Dr. E., JCI Member
*3 Graduate student, Graduate School of Civil Engineering, Tokyo Institute of Technology, JCI Member
*4 Manager, Research and Development Center, DPS Bridge Works Co., Ltd., Dr. E., JCI Member

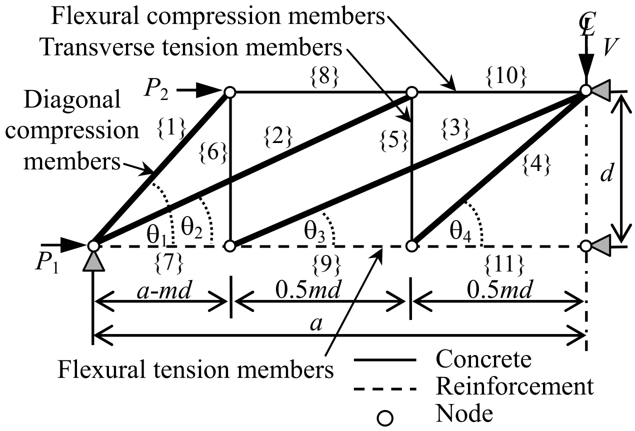

Fig. 1 Schematic diagram of the simplified truss model

of the horizontal distance of the diagonal compression member {3} is adopted. From the parametric study of the externally prestressed concrete beams, the equation for estimating the value of m can be expressed as the following:

$$m = 1.3\left[\left(1 + 0.2\frac{\sigma_u}{\sigma_u + \sigma_l}\right)\frac{\sigma_l}{k}\right]^{-\frac{2}{3}}\left(\frac{a}{d}\right)^{\frac{2}{5}}\left(\frac{f_c'}{k}\right)^{\frac{1}{3}} \tag{1}$$

where k is a constant equal to 1 N/mm^2 for making m dimensionless, σ_u is the upper extreme fiber stress (N/mm^2), σ_l is the lower extreme fiber stress (N/mm^2), f_c' is the compressive strength of concrete (N/mm^2).

By considering the effects of bearing plates and effective depth, the values of the horizontal thickness in the vicinity area of a loading point, t_l, and support, t_s, are expressed in Eqs. 2 and 3.

$$t_s = (w_l + 0.1d)\left(\frac{b_f}{b_w}\right)^{\frac{1}{5}}\left(1 + \sqrt{\frac{A_s}{b_w d}}\right)\left(1 + \left(\frac{A_{sv}}{b_w s}\right)^{\frac{1}{4}}\right) \tag{2}$$

$$t_s = 2(w_s + 0.1d)\left(\frac{b_f}{b_w}\right)^{\frac{1}{5}}\left(1 + \sqrt{\frac{A_s}{b_w d}}\right)\left(1 + \left(\frac{A_{sv}}{b_w s}\right)^{\frac{1}{4}}\right) \tag{3}$$

where, w_l is the loading plate width; w_s is the support plate width; b_f is the width of flange; b_w is the width of web; A_s is the cross sectional area of longitudinal bonded tensile reinforcement; A_{sv} is the cross sectional area of stirrup; s is the spacing of stirrups. In the model, the members {1} – {2}, and members {3} – {4} in Fig. 1 are considered to be affected by support and loading plates, respectively. The cross sectional area of each strut member can be computed as the values of t_l or t_s multiplied with b_w and its inclination.

The resistance capacity of each diagonal compression member, R_i, can be obtained from f_c' incorporating the concrete softening parameter, η, the cross sectional area, A_i, and the inclination of each member (according to the result from Eq. 1) as the following expression.

$$R_i = \eta f_c' A_i \sin\theta_i \tag{4}$$

In order to calculate the shear carrying capacity of externally prestressed concrete beams, the equivalent elastic analysis is applied. That is, after computing the value of m (Eq. 1), each member force, F_i, caused by the externally applied shear force, V, can be determined by employing the Castigliano's second theorem. After obtaining the member force, F_i, the shear carrying capacity can be estimated by comparing F_i with R_i. One of struts becomes critical when F_i/R_i becomes greater or equal to 1.0.

Although the simplified truss model [1] is proven to provide simplicity and high accuracy in the prediction on the shear carrying capacity of externally prestressed concrete beams, it has not yet been extended to the segmental concrete beams. Because of the discontinuity of segmental concrete beams, the behavior of stress flow or shear transfer inside segmental concrete beams may be different from externally prestressed concrete monolithic beams. This may lead to the shortcoming of the simplified truss model, which is based on the stress flow concept.

3. EXPERIMENTAL PROCEDURES

The test specimens consisted of two segmental concrete beams prestressed with external tendons, with the same total length at 3.5 m, cross section dimensions and reinforcement details as shown in Fig. 2. The specimens were named as H40 and H80 as tabulated in Table 1. The main parameter was the segmental length. The design effective prestress in terms of the lower extreme fiber stress, σ_l, was set to 19 N/mm^2. The actual values of effective prestress are shown in Table 1.

3.1 Materials

In all specimens, the internal longitudinal tensile reinforcement consisted of six deformed steel bars with nominal diameter of 13 mm (A_s = 126.7 mm^2), eight deformed steel bars are for longitudinal compressive reinforcement with nominal diameter of 10 mm (A_s' = 71.33 mm^2). Transverse reinforcement with a nominal diameter of 6 mm (A_v = 63.34 mm^2) was provided in web and flange throughout the length of beams with the spacing, s, of 400 mm and 100 mm, respectively. Their average yield strength, f_y, average tensile strength, f_u, modulus of elasticity, E_s, are illustrated in Fig. 2. For external tendons, two straight 19-wire prestressing tendons with a nominal diameter of 17.8 mm (A_{ps} = 208.4 mm^2) were prepared at the bottom and top layers as external tendons. The yield strength, f_{py}, the tensile strength, f_{pu}, and the modulus of elasticity of external tendons, E_{ps}, were 1680 N/mm^2, 1900 N/mm^2 and 191.3 kN/mm^2, respectively.

The match-cast technique was utilized in this

Table 1 Details of test beams

Beams	L^{*1}	σ_u^{*2}	σ_l^{*3}	$f_c'^{*4}$ for batch A	$f_c'^{*4}$ for batch B	f_t^{*5} for batch A	f_t^{*5} for batch B
H40	400	0.1	18.5	69.7	65.5	4.3	4.2
H80	800	0.0	19.6	61.8	69.7	4.1	4.4

Note: *1 Segmental length (mm)
*2 Upper extreme fiber stress (N/mm^2)
*3 Lower extreme fiber stress (N/mm^2)
*4 Compressive strength of concrete (N/mm^2)
*5 Tensile strength of concrete (N/mm^2)

Table 2 Mix proportion of concrete

W/C %	s/a %	W^{*1} (kg)	C^{*2} (kg)	S^{*3} (kg)	G^{*4} (kg)	SP^{*5} (kg)
43	54.5	168	395	934	792	2.17

Note: *1 Water
*2 Cement, density = 3.14 g/cm^3
*3 Fine aggregate, density=2.60g/cm^3, F.M.=2.67
*4 Coarse aggregate, density=2.64g/cm^3, F.M.=6.67, G_{max}=20mm
*5 Super-plasticizer, density=1.05g/cm^3

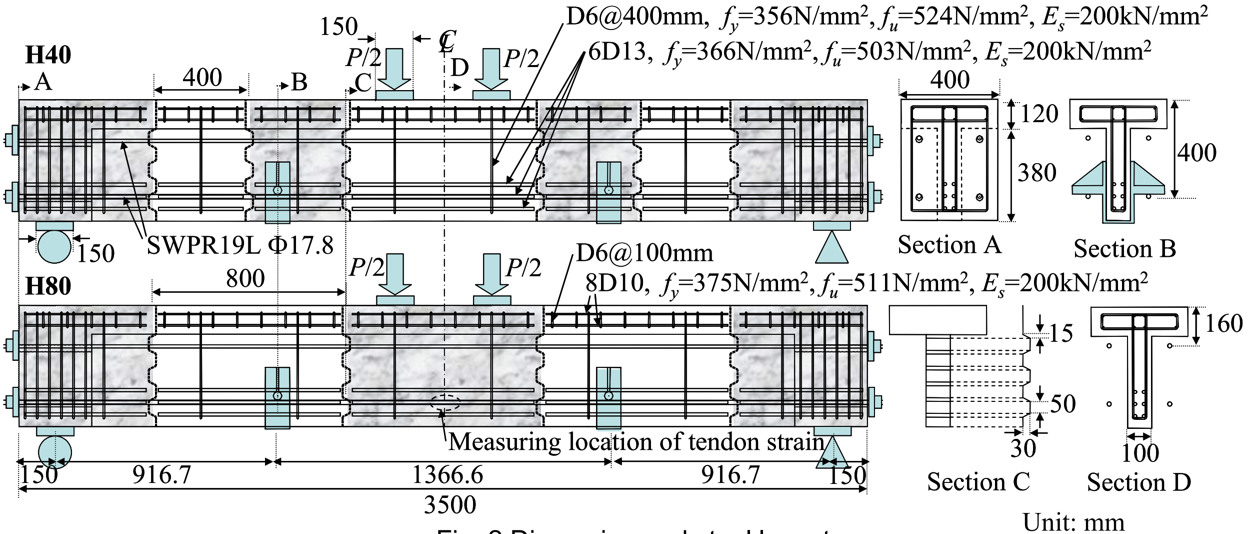

Fig. 2 Dimension and steel layout

study; therefore, the concrete was cast for two times in each segmental beam with the same mix proportion as shown in Table 2. Firstly, the batch A, shaded area in Fig. 2, was cast. After hardening of batch A, the formwork was removed and prepared for batch B, unshaded area. The actual compressive and tensile strengths of concrete in each batch were measured on the day of testing, and tabulated in Table 1. The compressive and tensile strengths of epoxy, used at segmental joints, were more than 60 N/mm^2 and 12.5 N/mm^2, respectively.

3.2 Experimental Setup

Before testing, the beam specimens were prestressed using symmetrically arranged external tendons on both sides of the section deviated at 916.7 mm from the supports by two deviators and anchored at the ends of beams. The strain of the prestressing tendon was taken as its average value of three electrical strain gauges, placed on the tendons at the midspan. All beams had straight tendon profiles, with an effective depth of 400 mm at the midspan for the bottom layer, and 160 mm for the top layer. The tendons were stressed as indicated by σ_u and σ_l in Table 1.

Deflections at the midspan and deviators, crack width, joint opening, prestressing force in external tendons and strains of concrete, steel and tendon were measured and monitored in each beam. The beams were simply supported over a span of 3.2 m and two-point symmetrical loading with a distance between loading points of 400 mm was provided. The shear span was set to 1.4 m and the effective depth was 400 mm (i.e. shear span to effective depth ratio, a/d, was 3.5). The 150 mm width of loading and support plates were used in the test.

4. FEM ANALYSIS

The nonlinear FEM using DIANA system has been conducted to examine the shear failure mechanism of segmental prestressed concrete beams. Four node quadrilateral isoparametric plane stress elements in a two dimensional configuration were adopted for concrete as illustrated in Fig. 3. The interface elements used at the deviators and at the end anchorages are also shown in Fig. 3. The friction between the tendons and the deviators is neglected. The stiffness in n-axis, D_n, is set to be zero for tension due to the opening between the tendons and the deviators. For compression, due to the closing between the tendons and the deviators, the extremely large stiffness is applied as shown in Fig. 3. For t-axis, the stiffness, D_t, is set to be zero due to the assumption of no friction between the deviators and tendons. Because of its applicability and simplicity, the flat joint model [3] is applied at the segmental joints. The flat joint model is composed of two-node interface elements, with different constitutive laws depending on the real geometry of shear key that the elements were reproducing. The constitutive equation of the flat joint model is adopted from Turmo et al. [3] due to the

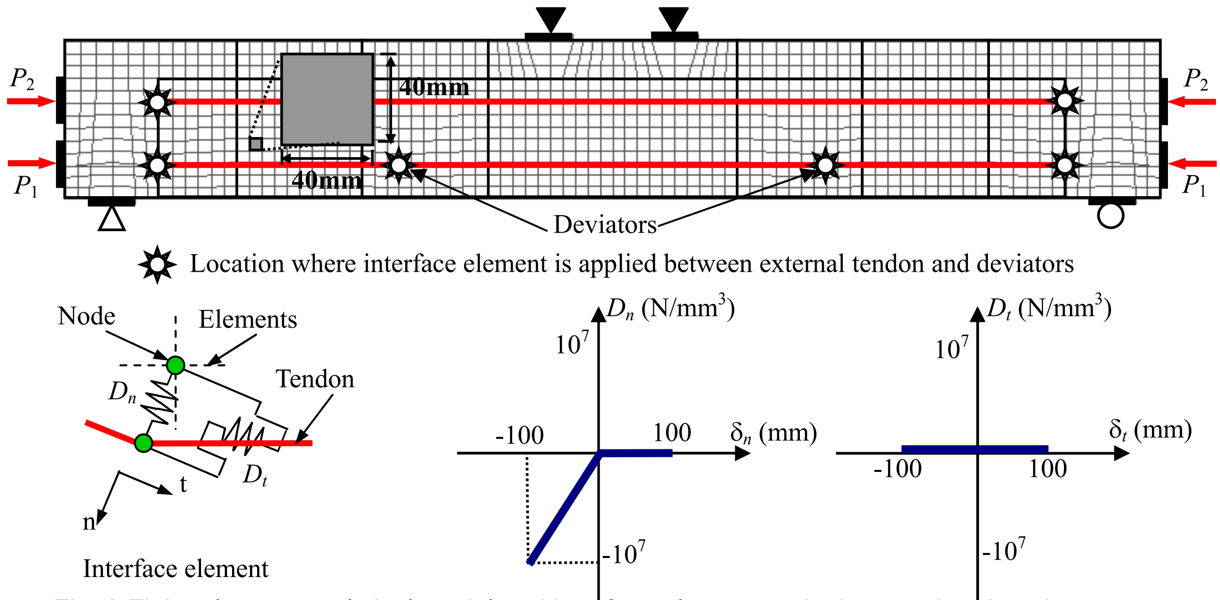

Fig. 3 Finite element analytical model and interface element at deviator and end anchorage

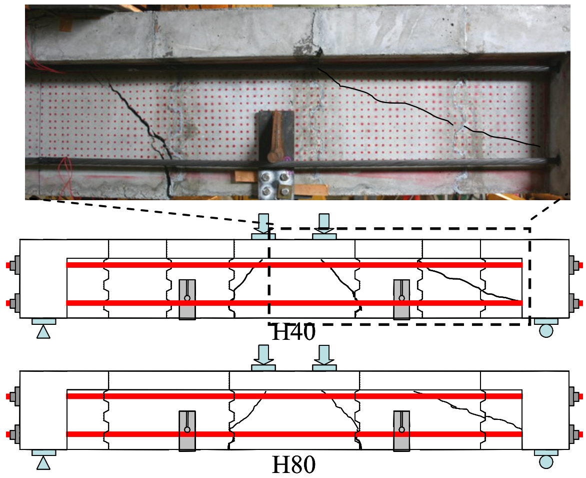

Fig. 4 Crack patterns

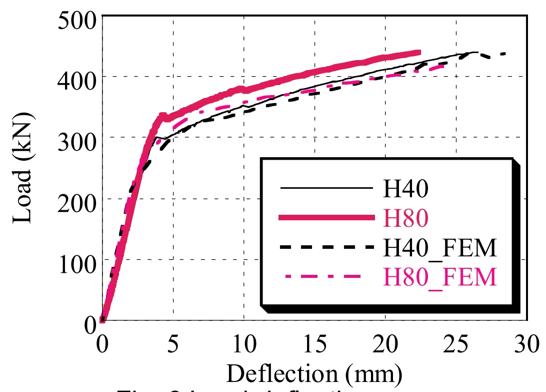

Fig. 6 Load-deflection response

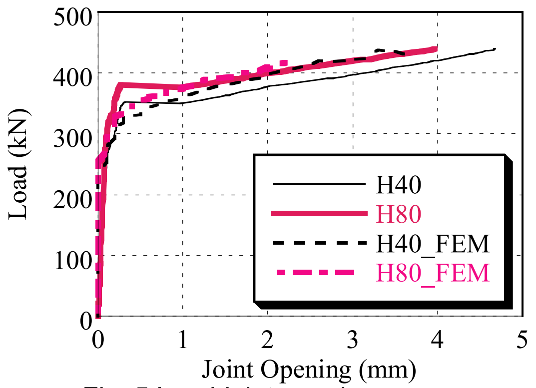

Fig. 5 Load-joint opening response

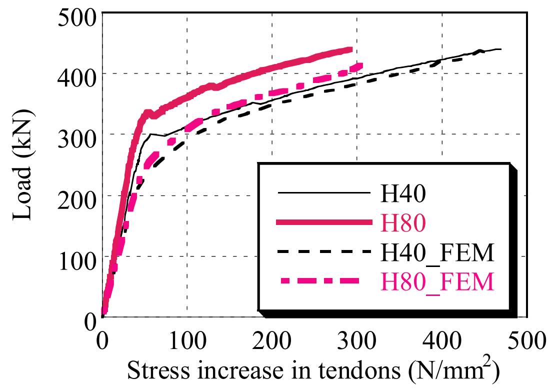

Fig. 7 Load-stress increase response

similar dimension of shear keys. Since the cracking observed in the experiment corresponded to the development of one single crack that accumulates all the deformations, a discrete crack model is selected as a model for the interface elements at segmental joints. The elastic stiffness matrix, D_n and D_t, had a sufficiently high values, 10^7 N/mm^3, in order to model the continuous geometry (i.e. before joint opening). The tensile strength of the concrete, f_t, was obtained from the experiment. The value of fracture energy, G_F, was found by considering the average compressive strength of concrete and the maximum size of the aggregate as recommended by JSCE specification [4].

In the analysis, the smeared crack model is adopted as the crack model to concrete elements. For the constitutive model in compression, Thorenfeldt's model [5] is applied. After cracking, the tension softening model proposed by Hordijk [6] is utilized as the concrete constitutive model under tension. Two node truss elements are applied for the tendon elements.

Table 3 Summary of experimental and calculated results

Beams	Joint opening (mm)	P_{joint} *1 (kN)	δ_u *2 (mm)	f_{ps} *3 (N/mm^2)	d_{pu} *4 (mm)	P_u *5 (kN)	$P_{u,Mcr}$ *6 (kN)	$P_{u,\,Sim.}$ *7 (kN)	$P_{u,\,FEM}$ *8 (kN)
H40	4.7	298	27	1341	388	439	332	385	442
H80	4.0	329	28	1204	389	440	336	352	417

Note: *1 Loading resistance at joint opening
*2 Midspan deformation at peak
*3 Tendon stress at peak
*4 Bottom tendon level from upper fiber
*5 Peak resistance from experiment
*6 Peak resistance from M_{cr} method
*7 Peak resistance from simplified truss model
*8 Peak resistance from FEM

Table 4 Joint opening from FEM

Beams	Joint opening (mm), Fig. 8		
	Joint A	Joint B	Joint C
L1	0.0	0.0	3.7
L2	0.0	0.3	4.9
L3	0.5	2.2	5.4
L4	5.9	8.1	12.3

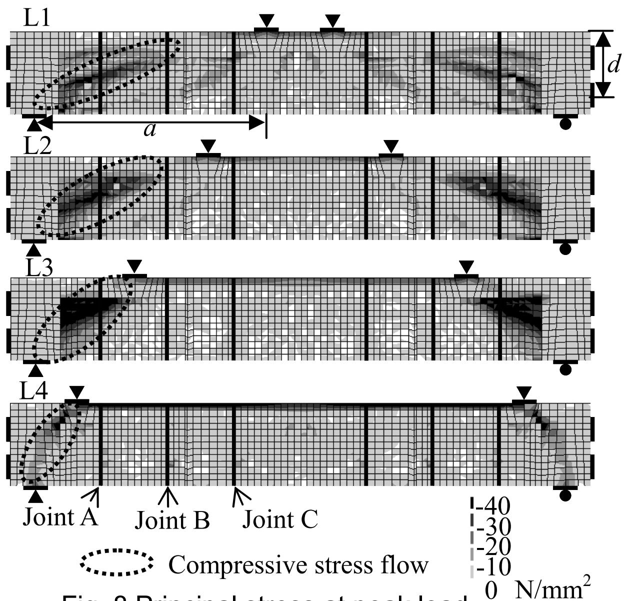

Fig. 8 Principal stress at peak load

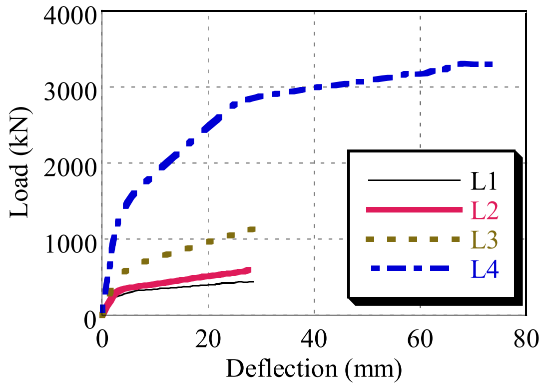

Fig. 9 Load-deflection response from FEM

These truss elements are connected to the concrete only at the deviators and end anchorages by means of using the interface element as shown in Fig. 3. The reinforcement was modeled by means of embedded reinforcement elements. The bilinear elasto-plastic model of steel is adopted for the longitudinal reinforcement and prestressing tendons. During the analysis, the prestressing force is applied by using the incorporated prestressing command in DIANA system at the first step. After the first step, the displacement control and the Quasi-Newton method (secant method) is used for the iteration.

5. RESULTS AND DISCUSSION

5.1 Crack Patterns and Joint Opening

The crack patterns are depicted in Fig. 4. There was no flexural crack that could be observed in flexure span (between two loading points). However, the vertical crack in the shear span near to the locations of segmental joint, where are next to the loading points, could be observed after the diagonal cracks occurred from the loading points to the locations of segmental joint as shown in Fig. 4. As the load increased, the vertical crack next to the segmental joints opened (joint opening). These joint openings were measured at the lower extreme fiber between each segments, and plotted as shown in Fig. 5. After the joint opening, the only two joints at the midspan increased in width and propagate along the diagonal crack to the top flange. The loading was suddenly dropped due to the second diagonal crack near to the support, and the specimens failed in diagonal shear compression failure. It might be interesting to note that although the segmental joint opened, the shear force can transfer to the support. This will be discussed in Chapter 6.

5.2 Load-Deflection and Stress Increment

Figures 6 and 7 illustrate the responses of applied load versus deflection and load versus stress increase, respectively. The summary of measured data, which includes the load at joint opening, the peak load, the midspan deflection, the stress in external tendons and tendon depth at the peak, is tabulated in Table 3. At the beginning, the beams behaved as a linear elastic body. The increase in deflection and stress increment in external tendons were very small, until the sudden diagonal cracks can be observed at the middle segment near to the loading points. The load was slightly dropped and the vertical crack near to the segmental joints, which was close to the loading points, opened and the stiffness of the beams was reduced. After that the deflection increased with the small increase in load until the peak load resulting also in significant increase of stress increment in external tendons. At the peak load, the second sudden diagonal crack occurred near to the support, causing the sudden failure. From Figs. 6 and 7, it can be observed that specimens H40 and H80 have almost the same loading resistance. Therefore, it can be said that the segmental length has less significant effect to the shear carrying capacity.

The validation of nonlinear FEM is made by comparing the analytical results with the experimental results as shown in Figs. 5, 6 and 7. The nonlinear

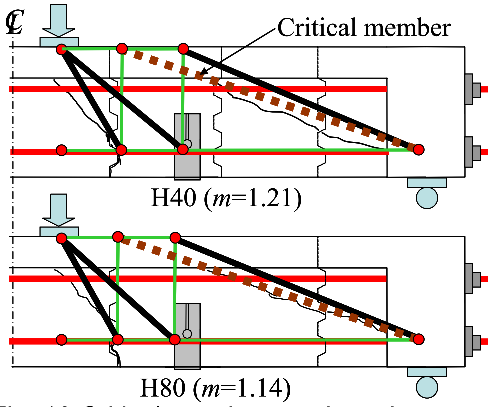

Fig. 10 Critical members and crack patterns

FEM can predict the load-deflection, load-stress increment and the load-joint opening responses of segmental prestressed concrete beams very well.

6. INFLUENCE OF LOADING POSITION ON SHEAR CARRYING CAPACITY

The nonlinear FEM is applied in order to investigate the influence of loading position on the compressive stress flow and shear carrying capacity in segmental prestressed concrete beams. The main parameter is the ratio of loading distance to span length, a/d, for 4 cases. Those are L1 (same as specimen H40), L2, L3 and L4, having a/d equal to 3.5, 2.6, 1.5 and 0.6, respectively. The dimensions and reinforcement layouts are the same with H40 (Fig. 2.)

Figure 8 shows the principal compressive stress at the peak load for those beams (L1, L2, L3 and L4) and Fig. 9 and Table 4 show the response between load and deflection and the joint opening in each segmental joint at the peak load, respectively. It is found that when the loading points move near to the support, the compressive stress flow transfers directly to the support; therefore, the beams can resist more shear force as illustrated in Fig. 9. Please note that when the load moved to the support, it leads to the change of a/d, which affects the shear carrying capacity of concrete beams. Because of the increase in shear carrying capacity of beam L4, this beam failed in flexure failure mode. From FEM analysis, it results that the joints located in the flexural span open significantly as tabulated in Table 4. On the other hand, the segmental joints located within the shear span remain nearly in contact, transferring the compressive stress to the support. Therefore, it is proven from this result that by moving the loads toward the supports, the compressive stress can still transfer to the supports.

7. COMPARISON WITH THE PREDICTION EQUATIONS

In this study, the shear carrying capacity of two beams from the experiment is used to confirm the applicability of the simplified truss model [1] and M_{cr} method [2]. In calculation of the simplified truss model, four diagonal compression members are considered. The number of diagonal compression member is demonstrated in Fig. 1. The typical crack patterns from the experiments at the ultimate stage are utilized to compare with the critical members in the simplified truss model as illustrated in Fig. 10. The bold dashed line in Fig. 10 represents the critical member of each case. From these comparison results, it is proven that the simplified truss model is applicable for predicting the location of the critical crack of segmental prestressed concrete beams. Moreover, the comparisons for shear carrying capacity of the experimental results with the calculated results, as shown in Table 3, show that the simplified truss model yields reasonable accuracy and reliability in prediction with an average value (AVE.) of P_u/P_{CAL} of 1.20, while the AVE. of P_u/P_{CAL} of M_{cr} method is 1.32.

8. CONCLUSIONS

(1) The segmental length has less effect to the shear carrying capacity of the beams according to the experimental and analytical results in this study.
(2) The analytical model of nonlinear FEM is applicable to examine the shear failure mechanism of segmental concrete beams.
(3) The loading position has less effect on the stress flow in segmental beams. If the segmental joints in shear span remain in contact, the compressive stress can transfer to the supports.
(4) The simplified truss model can provide good agreement with the experimental results.

ACKNOWLEDGEMENT

Sincere gratitude is expressed to Mr. Tsuyoshi Hasegawa, from DPS Bridge Works, Co., Ltd. for his assistance in conducting the experimental works.

REFERENCES

[1] Sivaleepunth, C. et al: Simplified Truss Model for Externally Prestressed Concrete Beams, JSCE Journal of Materials, Concrete Structures and Pavements, Vol. 63 (4), 2007, pp. 562-574
[2] Ito, T., Yamaguchi, T. and Ikeda, S.: Flexural Shear Behavior of Precast Segmental PC Beam, Proceedings of the JCI, Vol. 16, No.2, 1992, pp. 967-972 (in Japanese)
[3] Turmo, J., Ramos, G. and Aparicio, A.C.: FEM Modeling of Unbonded Post-tensioned Segmental Beams with Dry Joints, Engineering Structures, Vol. 28, 2006, pp. 1852-1863
[4] Japan Society of Civil Engineers (JSCE): Standard Specification for Concrete Structures (Structural Performance Verification), 2002
[5] Thorenfeldt, E., Tomaszewicz, A. and Jensen, J. J.: Mechanical Properties of High-strength Concrete and Applications in Design, Symposium Proceedings of Utilization of High-strength Concrete, Norway, 1987
[6] Hordijk, D. A.: Local Approach to Fatigue of Concrete, PhD thesis, Delft University of Technology, 1991